

Thermochemistry and Infrared Spectroscopy of Neutral and Cationic Iron–Polycyclic Aromatic Hydrocarbon Complexes of Astrophysical Interest: Fundamental Density Functional Theory Studies

Aude Simon* and Christine Joblin

Centre d'Etude Spatiale des Rayonnements, UMR 5187, Université Toulouse 3, Centre National de la Recherche Scientifique, 9 Av. du Colonel Roche, 31028 Toulouse Cedex 4, France

Received: March 30, 2007; In Final Form: July 20, 2007

This paper reports extensive calculations on the structural, thermodynamic, and mid-infrared spectroscopic properties of neutral and cationic model iron–polycyclic aromatic hydrocarbon (PAH) complexes of astrophysical interest for three PAHs of increasing size, namely, naphthalene ($C_{10}H_8$), pyrene ($C_{16}H_{10}$), and coronene ($C_{24}H_{12}$). Geometry optimizations and frequency calculations were performed using hybrid Hartree–Fock/density functional theory (DFT) methods. The use of DFT methods is mandatory in terms of computational cost and efficiency to describe the electronic and vibrational structures of such large organometallic unsaturated species that present several low-energy isomers of different structures and electronic and spin states. The calculated structures for the low-energy isomers of the model Fe–PAH and Fe–PAH⁺ complexes are presented and discussed. Iron–PAH binding energies are extracted, and the consequences of the coordination of iron on the infrared spectra of neutral and cationic PAHs are shown with systematic effects on band intensities and positions being demonstrated. The first results are discussed in terms of astrophysical implications. This work is the first step of an ongoing effort in our group to understand the photophysics and spectroscopy of iron–PAH complexes in the conditions of the interstellar medium using a synergy between observations, laboratory experiments, and theory.

1. Introduction

1.1. Astrophysical Context. In the early 1980s, Léger and Puget¹ and Allamandola et al.² suggested that polycyclic aromatic hydrocarbons (PAHs) and PAH-related molecules are the major carriers of the discrete emission infrared spectrum that is observed ubiquitously in the interstellar medium (ISM) in the 3–14 μm range. Since then, many studies, laboratory experiments,^{3–13} and theoretical calculations^{14–23} have been dedicated to the identification of the carriers of these features, the so-called aromatic infrared bands (AIBs) at 3.3, 6.2, 7.7, 8.6, 11.3, and 12.7 μm . There is now compelling evidence that these features are due to a complex mixture of ionized and neutral, possibly substituted/complexed PAHs of different sizes,^{24–34} but no satisfactory match to the observed spectra has been obtained yet.

Later on, Serra et al.³⁵ and Chaudret et al.³⁶ suggested that interstellar PAHs could coordinate efficiently to metal atoms. In particular, the important depletion of metallic iron from the gas phase could be partially accounted for by its coordination to PAHs to form stable complexes. The authors also suggested a catalytic role of the coordinated iron in the growing of carbon macromolecules.³⁷ The proposal by Serra et al. and Chaudret et al. motivated at the time a few experimental^{38,39} and theoretical^{40,41} studies on small iron–PAH systems. Klotz et al.⁴² established a correlation between metal–PAH binding energies and the depletion of metal atoms in the ISM. They modeled the photo-thermodissociation of organometallic species in the ISM and concluded that: (i) the abundance of metal–

PAH compounds would explain 5–10% of the depletion of metallic atoms in the gas phase in the diffuse interstellar medium and (ii) in the UV-irradiated regions of the ISM, a critical size for the stable complexes can be determined. The idea of the photodissociation of very small iron–PAH grains was also put forward by Rodríguez to account for the increased abundance of atomic iron in HII regions.⁴³ The size of these grains should be small enough ($a \approx 10 \text{ \AA}$) for fragmentation to occur after the absorption of one or two far-UV photons of typically 20 eV.

Finally, recent studies on the spatial distribution of the mid-IR spectra in reflection nebulae showed that the carriers of the AIBs are produced at the surface of molecular clouds by evaporation of very small grains (VSGs).^{32,44} Rapacioli et al. suggested that these VSGs are PAH aggregates, which can evaporate into PAH units.^{32,45} Following the proposal by Serra et al., our aim is to investigate the possible presence of iron in these clusters, which requires dedicated studies on their IR spectra and their photostability against UV photons. As a first step, we report in this paper the properties of several Fe–PAH complexes.

1.2. Metal–PAH Complexes in Physical Chemistry: Experiments and Calculations. The study of iron complexes with large PAHs in the gas phase is challenging both experimentally and theoretically. Pozniak and Dunbar reported the first kinetic study on the formation of Fe–($C_{24}H_{12}$)⁺ and Fe–($C_{24}H_{12}$)₂⁺ species by radiative association of M⁺ with $C_{24}H_{12}$ in the low-pressure conditions of an Fourier transform ion cyclotron resonance mass spectrometer (FTICRMS).⁴⁶ They showed in particular that Fe–($C_{24}H_{12}$)₂⁺ rapidly formed. Duncan and co-workers reported the formation of Fe_x–($C_{24}H_{12}$)_y⁺ ($x, y = (0-$

* Author to whom correspondence should be addressed. Phone: +33 5 61 55 75 47. Fax: +33 5 61 55 67 01. E-mail: aude.simon@ccsr.fr.

2,1–3) complexes in a molecular beam and their photofragmentation using lasers at 610, 532, and 355 nm.⁴⁷ They showed the dissociation of $\text{Fe}-(\text{C}_{24}\text{H}_{12})^+$ into $\text{Fe} + \text{C}_{24}\text{H}_{12}^+$ to be in line with the relative ionization potentials of iron and coronene. $\text{Fe}-(\text{C}_{24}\text{H}_{12})_y^+$, $y = (3,4)$ complexes were observed to photodissociate into $\text{Fe}-(\text{C}_{24}\text{H}_{12})_2^+$ and one or two coronene molecules, illustrating the high stability of the presumably sandwich structure of $\text{Fe}-(\text{C}_{24}\text{H}_{12})_2^+$. Interestingly, multimetal $\text{Fe}_2-\text{C}_{24}\text{H}_{12}^+$ and $\text{Fe}_3-\text{C}_{24}\text{H}_{12}^+$ complexes were shown to photodissociate into $\text{C}_{24}\text{H}_{12}^+$ and iron atoms, leading to the proposal that these species are atomic iron atoms individually interacting with the surface of coronene. However, this is not in agreement with the theoretical results obtained by Senapati et al.,⁴⁸ who found that the ground-state structure of $\text{Fe}_2-\text{C}_{24}\text{H}_{12}^+$ is an iron dimer coordinated to the coronene surface.

Experimental infrared spectroscopy studies on iron–PAH complexes are sparse. The spectra of neutral $\text{Fe}-\text{C}_{16}\text{H}_{10}$ and $\text{Fe}-\text{C}_{24}\text{H}_{12}$ complexes were recorded in rare gas matrices.⁴⁹ Infrared multiple photon dissociation (IRMPD) experiments on $\text{Fe}-\text{C}_6\text{H}_6^+$, $\text{Fe}-\text{C}_{10}\text{H}_8^+$, and $\text{Fe}-\text{C}_{13}\text{H}_{10}^+$ complexes formed in the cell of an FTICRMS were performed at the Free Electron Laser for Infrared Experiments (FELIX).⁵⁰ With this setup, we recently obtained the IRMPD spectra of $\text{X}-\text{Fe}-\text{C}_{24}\text{H}_{12}^+$ ($\text{X} = \text{C}_5\text{H}_5$ or $\text{C}_5(\text{CH}_3)_5$) complexes in the gas phase.⁵¹

Before the development of methods based on density functional theory (DFT), the size of the systems for which the electronic structure could be investigated was very restricted. The electronic structures and infrared spectra of C_{10}H_8 , $\text{C}_{14}\text{H}_{10}$, and $\text{C}_{16}\text{H}_{10}$ were studied with the more basic and approximate *ab initio* method, Hartree–Fock, by Ellinger and collaborators.^{15,16,20,21} They studied in particular the effect of ionization and dehydrogenation on the IR spectra of small PAHs. They showed that for the above species ionization has a drastic effect on the intensity ratios, significantly decreasing the $I(3.3 \mu\text{m})/I(6.2 + 7.7 \mu\text{m})$ ratio, in agreement with astronomical observations.¹⁵ They also studied the effect of double ionization on pyrene and performed the first (basic) calculations on an isomer of the $\text{Fe}-\text{C}_{14}\text{H}_{10}^+$ complex.¹⁶ Due to the limitation in the size of the systems that could be treated using “classical” *ab initio* methods, it was always assumed that the results obtained on small PAHs could be extrapolated to larger ones. DFT methods are now currently used. They allow for a faster exploration of potential energy surfaces (PESs). Systematic studies therefore have been performed on larger PAHs^{18,23,52} and metallic complexes involving coronene ($\text{C}_{24}\text{H}_{12}$)^{48,53,54} or corannulene ($\text{C}_{20}\text{H}_{10}$).^{53,55}

In this work, we make use of hybrid Hartree–Fock/DFT methods to calculate the structures and thermodynamics of neutral and cationic iron–PAH complexes as well as their IR spectra. We aim at exploring these properties for three PAHs of increasing size, namely, naphthalene (C_{10}H_8), pyrene ($\text{C}_{16}\text{H}_{10}$), and coronene ($\text{C}_{24}\text{H}_{12}$). First astrophysical implications are given, emphasizing two aspects: (i) the stability of these systems and (ii) the influence on the IR spectra of the coordination of iron on PAHs in relation to the interpretation of the astronomical IR spectra.

2. Methods

The description of electronic and vibrational structures of large unsaturated organometallic systems remains challenging. The large size of these species and the large number of geometries and spin states to consider make the use of DFT methods mandatory. For geometry optimizations and harmonic vibrational mode calculations, we used two hybrid Hartree–

Fock/DFT functionals that have been widely employed for unsaturated organometallic complexes.

A first series of calculations was performed using the Becke–3 Lee–Yang–Parr (B3LYP)⁵⁶ functional with a relativistic double- ζ effective core potential LanL2dz.⁵⁷ The B3LYP functional is probably the most widely used functional to describe complexes with transition metals. For example, structures, binding energies, and vibrational frequencies for such complexes containing water, acetylene, ethylene, C_{12}H_6 , and coronene were obtained with this method.⁵⁴ Besides, from our experience, a good agreement was found between IR spectra calculated with the B3LYP method and IRMPD experimental spectra for iron–alkene complexes.⁵⁸ The first systematic study on the IR spectra of a series of neutral, cationic, and anionic PAHs ranging from naphthalene to ovalene using the B3LYP functional was done by Langhoff.¹⁸ The B3LYP method was also chosen to establish a spectroscopic database for PAHs.²³ The LanL2dz basis set was used to obtain rapidly a first set of structures and spectra. A similar level of calculations has been used recently to calculate electronic structures and thermodynamic properties of large metal-containing clusters such as metalloboranes and metallo-carboranes,⁵⁹ onion-like inorganic fullerenes $[\text{X}@\text{Y}_{12}@\text{Z}_{20}]^\alpha$ ($\text{X} = \text{As}, \text{Ge}$; $\text{Y} = \text{Ni}, \text{Zn}$; $\text{Z} = \text{As}, \text{Ge}$, $\alpha = 0, +1, -3$),⁶⁰ and inorganic cage molecules encapsulating Kr.⁶¹

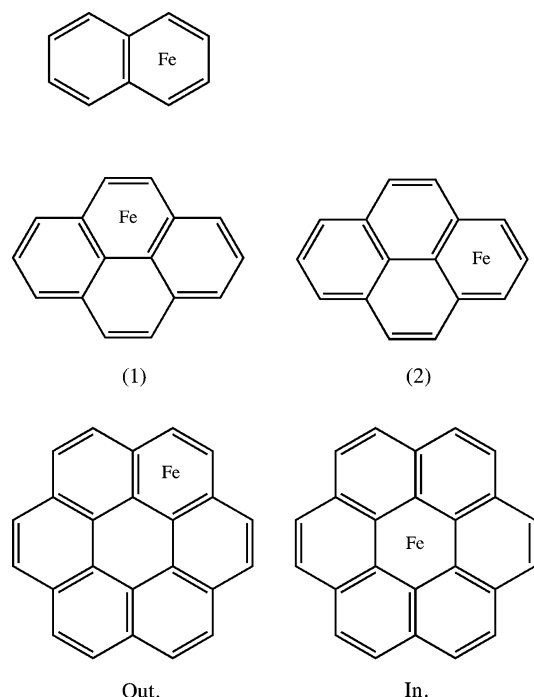
Optimization and harmonic frequency calculations were also performed using the hybrid functional MPW1PW91^{62,63} and the 6-31+G(d,p) basis set, which has been used recently to calculate infrared spectra of cationic iron–benzene, –naphthalene, and –pyrene complexes.⁵⁰ The performances of B3LYP and MPW1PW91 to calculate binding energies were compared for metal–ion complexes of benzene, and the MPW1PW91 functional was found to provide results in slightly better agreement with experiment,⁶⁴ although the difference was not drastic. In the same vein, a difference of 1.5 kcal/mol was found in the binding energies of cationic metal–corannulene and metal–coronene complexes using the two functionals.⁵³ Scarce experimental data are available on such systems, and the calculations suffer in general from a lack of calibration.

In the following, the B3LYP/LanL2dz level of calculations will be designated as MB1, and the MPW1PW91/6-31+G(d,p) one as MB2. Only structures with iron–PAH π -type interactions were considered. In most cases of interaction between a metal cation and a planar π -system, the most favorable binding site for the metal cation is η^6 over one of the six-membered rings.⁵³ For all starting point geometries the iron atom was therefore located on top of the middle of an aromatic ring. These are reported on Scheme 1. In the case of iron–naphthalene complexes, only one type of isomer was considered as the two rings are equivalent. Isomers 1 and 2 were calculated for iron–pyrene, isomers “In” and “Out” for iron–coronene where the iron atom interacts with the inner ring or one of the outer rings, respectively.

Geometry optimizations and frequency calculations were performed with the Gaussian 03 program suite.⁶⁵ All possible spin multiplicities of the electronic structure of iron were considered.

3. Thermodynamics and Structures

3.1. Calibration. Errors in the calculated values of the binding energies can come from uncertainties inherent to DFT methods and the finite character of the basis set. To gain some insights into the possible sources of errors, some test calculations were performed on ionization potentials (IPs) of iron and PAHs and atomic excitation energies of Fe and Fe^+ relevant to this work.

SCHEME 1: π -Interaction Sites of Iron on Naphthalene, Pyrene, and Coronene


These values are compared with the most recent experimental ones available in the literature (cf. Table 1).

The calculated values of the IPs were found to be lower than the experimental ones. For PAHs, the discrepancies range from -0.29 to -0.24 eV at the MB2 level and from -0.38 to -0.34 eV at the MB1 level. For iron, a larger discrepancy was found at the MB2 level (-0.57 eV) than at the MB1 level (-0.44 eV). The most relevant values for calibration are the relative IPs of PAHs and iron because we are interested in the relative energies of $\{\text{Fe}^+ + \text{PAH}\}$ and $\{\text{Fe} + \text{PAH}^+\}$ to find the lowest-energy asymptote from which the adiabatic binding energies are calculated. The computed differences of IPs between PAHs and iron ($\Delta\text{IP} = \text{IP}(\text{PAH}) - \text{IP}(\text{Fe})$) are reported in Table 1. The IPs of coronene and pyrene are found to be lower and the IP of naphthalene to be larger than that of iron, the discrepancy with experiment ranging from 0.22 to 0.33 eV at the MB2 level and from 0.10 to 0.19 eV at the MB1 level. Both levels of calculation provide the right relative order compared to experimental data, the best agreement being achieved at the MB1 level.

DFT methods are well-known to overestimate the stability of the d^n configuration of the metallic center over the d^{n-1} one. This is indeed observed for both Fe and Fe^+ at the MB1 level and, to a smaller extent, at the MB2 level (Table 1). The relative energy of the ${}^3\text{F}_4$ [$3d^7(4\text{F})4s^1$] state of iron versus its ${}^5\text{D}_4$ [$3d^6-4s^2$] ground state is found to be underestimated by 0.64 eV at the MB2 level and 1.07 eV at the MB1 level with respect to the experimental value (1.48 eV). This suggests that for Fe-PAH complexes the relative energies between their triplet and quintet spin states have to be regarded with caution especially at the MB1 level. In the same way, the relative energy of the ${}^4\text{F}_{9/2}$ [$3d^7$] state of Fe^+ versus its ${}^6\text{D}_{9/2}$ [$3d^6({}^5\text{D})4s^1$] ground state is underestimated by 0.14 eV at the MB2 level and 0.62 eV at the MB1 level with respect to the experimental value (0.23 eV). In the case of Fe-PAH $^+$ complexes, one therefore has to be careful when comparing the relative energies of the sextet and quartet spin states. From these results on the atomic excitation energies of Fe and Fe^+ , we conclude that the MB2 level is expected to better describe the relative energies of the lowest-

energy isomers of Fe-PAH and Fe-PAH $^+$. This level of calculation was found to be optimum after several tests on the atomic excitation energies using other basis sets.

Because of the finite character of the basis set, basis set superposition errors (BSSEs) introduce uncertainties on the absolute binding energies. Dunbar suggested that it could contribute to an uncertainty of $2-4$ kcal/mol ($0.1-0.2$ eV) on the absolute binding energies of metal-coronene and -coranulene complexes at a level of calculation similar to MB2.⁵³ An order of magnitude for the BSSE can be estimated using the counterpoise method.^{66,67} We used this method as it is implemented in the Gaussian code to estimate the BSSE corrections for all of the ground states of the Fe-PAH complexes. They were found to range from 0.34 to 0.68 eV at the MB1 level and from 0.07 to 0.32 eV at the MB2 level. These values have to be regarded with caution. They are more an indication of the magnitude of the BSSE, actually an overestimation of it, than an accurate compensation for it. In some cases, the reliability of these calculated values has been questioned.⁶⁸

We found that the MB2 level improves the quality of the results with respect to the MB1 level in regards to both the atomic excitation energies of the metallic atom and the BSSE. At the MB2 level, we can reasonably assume that the absolute binding energies are reliable within a maximum uncertainty of ~ 0.3 eV and the relative energies between similar spin states within less than 0.1 eV. Unless otherwise specified, only the results obtained at the MB2 level will be presented in the following for the sake of clarity. They will only be compared with the results obtained at the MB1 level in the aim of computations on larger systems.

3.2. Results. The calculated relative enthalpies at 0 K ($\Delta H(0$ K)) of the low-energy isomers of Fe-PAH and Fe-PAH $^+$ (PAH = C_{10}H_8 , $\text{C}_{16}\text{H}_{10}$, or $\text{C}_{24}\text{H}_{12}$) with respect to the most stable dissociation products $\{\text{Fe}({}^5\text{D}) + \text{PAH}\}$ and $\{\text{Fe}({}^5\text{D}) + \text{PAH}^+\}$ are reported in Table 2. As expected for these unsaturated organometallic complexes, an important density of low-energy isomers was found. Bond dissociation energies (BDEs) correspond to $-\Delta H(0$ K) values.

The most stable structures for neutral FePAH complexes were found to be in a quintet spin state. In the particular case of $\text{FeC}_{10}\text{H}_8$ the lowest-energy triplet and quintet spin states were found nearly degenerate as the ${}^5\text{A}''$ state lies only 0.04 eV above the ${}^3\text{A}''$ one. Given the fact that the MB2 level overestimates the stability of the ${}^3\text{F}_4$ state of iron with respect to its ${}^5\text{D}_4$ ground state, it is more likely that the ${}^5\text{A}''$ state is the effective ground state. As discussed in section 4, the two isomers can be distinguished by their infrared spectra. For Fe- $\text{C}_{24}\text{H}_{12}$, our results contrast with the ones obtained by Senapati et al., who determined that the ground state of Fe- $\text{C}_{24}\text{H}_{12}$ was a triplet spin state using a similar level of theory as the one used in this work.⁴⁸ Although triplet and quintet spin states are found in the ranges of 0.04 eV for Fe- C_{10}H_8 , 0.45 eV for Fe- $\text{C}_{16}\text{H}_{10}$, and 1.04 eV for Fe- $\text{C}_{24}\text{H}_{12}$, Fe-PAH complexes in singlet spin states lie higher in energy and were not found to be stable (BDE < 0). That was expected given the relative energy of the ${}^1\text{G}_4$ electronic state of iron with respect to its ground state ($+3.68$ eV; cf. Table 1).

When the size of the PAH increases from naphthalene to coronene, the BDE of neutral Fe-PAH complexes hardly changes (0.64 eV for ${}^3\text{A}''$ Fe- C_{10}H_8 , 0.68 eV for ${}^5\text{A}'$ Fe- $\text{C}_{16}\text{H}_{10}$, and 0.62 eV for ${}^5\text{A}'$ Fe- $\text{C}_{24}\text{H}_{12}$). A typical value of 0.6 eV could then be used as a standard value for the binding energy between iron and a neutral PAH. The value of 0.62 eV

TABLE 1: Comparison of Ionization Potentials (IPs) of Naphthalene, Pyrene, Coronene, and Iron, Relative IPs of PAHs and Fe, and Atomic Excitation Energies of Fe and Fe⁺ Relevant to This Work, Calculated at the B3LYP/lanl2dz (MB1) and MPW1PW91/6-31+G(d,p) (MB2) Levels, with the Most Recent Experimental Values^{79,80 a}

	IP(eV)			Δ IP(PAH-Fe)(eV)			electronic states of Fe	atomic excitation energies			electronic states of Fe ⁺	atomic excitation energies		
	MB1	MB2	expt. ⁷⁹	MB1	MB2	expt. ⁷⁹		MB1	MB2	expt. ⁸⁰		MB1	MB2	expt. ⁸⁰
naphthalene (C ₁₀ H ₈)	7.78	7.85	8.12 ± 0.02	0.30	0.50	0.20								
pyrene (C ₁₆ H ₁₀)	7.05	7.13	7.4256 ± 0.0006	-0.43	-0.22	-0.50	¹ G ₄ 3d ⁷ (² G) 4s ¹	+2.87	+3.68	+3.05	² G _{9/2} 3d ⁷	+1.47	+1.47	+1.97
coronene (C ₂₄ H ₁₂)	6.91	7.05	7.29	-0.44	-0.30	-0.63	³ F ₄ 3d ⁷ (⁴ F) 4s ¹	+0.41	+0.84	+1.48	⁴ F _{9/2} 3d ⁷	-0.39	+0.09	+0.23
Fe	7.48	7.35	7.92				⁵ D ₄ 3d ⁶ 4s ²	0.0	0.0	0.0	⁶ D _{9/2} 3d ⁶ (⁵ D) 4s ¹	0.0	0.0	0.0

^a All values are expressed in eV.

TABLE 2: Relative Enthalpies of the Most Stable Neutral and Cationic Iron–Naphthalene (Fe–C₁₀H₈), Iron–Pyrene (Fe–C₁₆H₁₀), and Iron–Coronene (Fe–C₂₄H₁₂) Complexes Calculated at 0 K with Respect to the Corresponding Asymptotes {Fe + PAH} and {Fe + PAH⁺} at the B3LYP/Lanl2dz (MB1) and MPW1PW91/6-31+G(d,p) (MB2) Levels of Theory^a

systems	MB1 B3LYP/Lanl2dz			MB2 MPW1PW91/6-31+G(d,p)			systems	MB1 B3LYP/Lanl2dz			MB2 MPW1PW91/6-31+G(d,p)		
	isomer	electronic state	ΔH (0 K) (eV)	isomer	electronic state	ΔH (0 K) (eV)		isomer	electronic state	ΔH (0 K) (eV)	isomer	electronic state	ΔH (0 K) (eV)
Fe(⁵ D) + C ₁₀ H ₈ (¹ A _g)			0.0			0.0	Fe(⁵ D) + C ₁₀ H ₈ ⁺ (² A _u)			+0.11			+0.50
							Fe ⁺ (⁶ D) + C ₁₀ H ₈ (¹ A _g)			0.0			0.0
Fe–C ₁₀ H ₈		¹ A'	-0.03	¹ A'	+0.94		Fe–C ₁₀ H ₈ ⁺	² A'	-1.46	² A'	-1.42		
		³ A''	-0.05	⁵ A''	-0.60			⁶ A'	-1.93	⁶ A'	-2.04		
		⁵ A''	-0.56	³ A''	-0.64			⁴ A''	-2.85	⁴ A''	-2.77		
							Fe ⁺ (⁶ D) + C ₁₆ H ₁₀ (¹ A _g)			+0.84			+0.22
Fe(⁵ D) + C ₁₆ H ₁₀ (¹ A _g)			0.0			0.0	Fe(⁵ D) + C ₁₆ H ₁₀ ⁺ (² B _{1g})			0.0			0.0
Fe–C ₁₆ H ₁₀	1	¹ A'	+1.67	1	¹ A'	+1.76	Fe–C ₁₆ H ₁₀ ⁺	1	² A'	-0.60	2	² A''	-0.98
	2	¹ A	+1.52	2	¹ A	+1.26		2	² A''	-0.79	1	² A'	-1.50
	2	⁵ A	+0.23	1	³ A''	-0.23		1	⁶ A'	-1.38	2	⁶ A''	-1.86
	2	³ A''	-0.21	2	⁵ A	-0.52		2	⁴ A	-1.42	1	⁶ A'	-1.90
	1	³ A''	-0.43	2	³ A''	-0.61		2	⁶ A''	-1.49	1	⁴ A'	-2.54
	1	⁵ A'	-0.70	1	⁵ A'	-0.68		1	⁴ A'	-2.30	2	⁴ A	-2.60
							Fe ⁺ (⁶ D) + C ₂₄ H ₁₂ (¹ A _g)			+0.97			+0.30
Fe(⁵ D) + C ₂₄ H ₁₂			0.0			0.0	Fe(⁵ D) + C ₂₄ H ₁₂ ⁺ (² A _u)			0.0			0.0
	In	¹ A ₁	+2.38	Out	¹ A'	+1.44		In	² A ₁	0.01	In	² A ₁	-0.33
	Out	¹ A'	+1.74	Out	¹ A'	+1.44		Out	² A'	-0.60	Out	² A'	-1.04
	In	³ A	+0.61	In	³ A	+0.76	Fe–C ₂₄ H ₁₂ ⁺	In	⁶ A	-1.23	In	⁶ A	-1.71
Fe–C ₂₄ H ₁₂	Out	³ A'	0.0	Out	³ A'	-0.37		Out	⁶ A''	-1.46	In	⁴ A	-1.91
	In	⁵ A	-0.56	In	⁵ A ^b	-0.05 ^b		In	⁴ A	-2.08	Out	⁶ A''	-2.03
	Out	⁵ A'	-0.61	Out	⁵ A'	-0.62		Out	⁴ A''	-2.30	Out	⁴ A''	-2.59

^a All values are expressed in eV. The electronic state of each isomer is specified. ^b The optimized structure was found to be a transition state.

obtained for ⁵A' Fe–C₂₄H₁₂ is in agreement with the value calculated by Senapati et al. (0.58 eV).⁴⁸ Interestingly, the values obtained at a lower level of theory (MB1) are becoming closer to the ones obtained at the MB2 level as the size of the PAH increases (Table 2): 0.56 vs 0.64 eV for Fe–C₁₀H₈, 0.70 vs 0.68 eV for Fe–C₁₆H₁₀, and 0.61 vs 0.62 eV for Fe–C₂₄H₁₂. This is encouraging for the study of the thermodynamics of larger neutral iron–PAH systems such as Fe–(C₂₄H₁₂)₂, for example, for which it is important that MB1 can provide reliable thermodynamic results, as a more accurate method would be too costly in computational time and memory.

Cationic iron–PAH complexes in doublet, sextet, and quartet spin states were found to have positive BDEs. An examination of the Mulliken charges on the iron atom and the PAH molecule shows that the positive charge is mainly localized on the PAH. All complexes in their ground states are in a quartet spin state as for the iron–benzene cation.¹⁴ The sextet spin states are

higher in energy, except for Fe–C₂₄H₁₂⁺ in which the quartet spin state associated with the “In” site lies 0.12 eV higher in energy than the sextet spin state associated with the “Out” site (cf. Scheme 1). As expected given the relative energy of the ²G_{9/2} state of Fe⁺ with respect to its ⁶D_{9/2} ground state (+1.47 eV, cf. Table 1), the doublet spin states of Fe–PAH⁺ complexes were found to be higher in energy (Table 2). The geometries and relative energies of Fe–C₂₄H₁₂⁺ obtained in this work differ from those obtained by Senapati et al., who found that the most stable isomer of Fe–C₂₄H₁₂⁺ was in a doublet spin state.⁴⁸

The BDEs for cationic complexes are larger than for the neutral complexes with a slight decrease with size; a binding energy of 2.77 eV was found for ⁴A'' Fe–C₁₀H₈⁺, 2.60 eV for ⁴A Fe–C₁₆H₁₀⁺, and 2.59 eV for ⁴A'' Fe–C₂₄H₁₂⁺. This suggests that a value of 2.6 eV could be used as a typical binding energy between iron and PAH cations larger than pyrene. The binding energies that we calculated for Fe–C₁₀H₈⁺ and Fe–

$C_{16}H_{10}^+$ (2.77 and 2.60 eV) are in line with those obtained by Szczepanski et al. at the same level of calculations (2.75 and 2.39 eV, respectively),⁵⁰ although the match is not perfect. The differences might result from different starting point geometries and/or different initial guesses for the orbitals, which may lead to a different minimum. This is due to the complexity of the theoretical treatment for the electronic structures of these unsaturated organometallic systems, which implies a large number of potential energy surfaces.

The BDE that we calculated for $Fe-C_{24}H_{12}^+$ (2.59 eV) is larger than the value obtained by Senapati et al.⁴⁸ (2.27 eV) and that obtained by Klippenstein and Yang⁵⁴ (2.42 eV). In the latter case, this is not surprising as the authors only considered the "In" site. Available experimental values as described below exhibit an overall agreement with theory. Pozniak and Dunbar concluded from association kinetic experiments in an FTICRMS that the BDE between a transition metal and coronene should be greater than 1.51 eV in the case of cationic systems.⁴⁶ Selective photodissociation experiments on mixed benzene-iron-coronene cations performed by Buchanan et al. led to the conclusion that the BDE of $Fe-C_{24}H_{12}^+$ should be superior to the BDE of $Fe-C_6H_6^+$,⁶⁹ whose experimental value was determined to be 2.15 eV in collision-induced dissociation experiments.⁷⁰ All of these experimental data are however not accurate enough to validate one theoretical model over the other.

As in the case of neutral complexes, there are differences in the calculated ΔH values between the MB2 and the MB1 levels. However, these differences are not so drastic and can be considered as acceptable for the purpose of obtaining information on larger systems for astrophysical models.

Although our prime interest is to quantify the energetics of Fe-PAH and Fe-PAH⁺ complexes, we also briefly describe the derived optimized structures for the ground states. These are reported in Figure 1. For all structures, we used starting point geometries with the iron atom on top of the center of an aromatic ring. In all cases, iron moved toward the periphery during the optimization process, leading to a final geometry belonging to the C_s group, or to the C_1 group in the particular case of $Fe-C_{16}H_{10}^+$. As can be seen in Figure 1, the distortion is slight in the case of the cations, the binding site of Fe keeping an η^6 coordination over one of the six-membered rings. For $Fe-C_{16}H_{10}^+$, structures 1 and 2 can be regarded as degenerate as a difference of 0.06 eV is not significant given the uncertainty of the method. Only structure 2 is reported in Figure 1. For $Fe-C_{24}H_{12}^+$, the coordination of iron to the outer ring is preferred by 0.68 eV to the one to the inner ring.

In the cases of $Fe-C_{16}H_{10}$ and $Fe-C_{24}H_{12}$, the iron atom is found to be located on top of the middle of an outer C-C bond, at 2.15 Å from the closest carbon atoms. It has an η^2 edge coordination, which is not observed for the higher-energy structures. This contrasts with the calculations by Senapati et al., who found that the ground state for $Fe-C_{24}H_{12}$ was a triplet spin state with the iron located on top of the middle of an outer ring.⁴⁸ The η^2 edge coordination is not common as a binding mode between transition metals and π systems. By studying the coordination of a series of transition metals to corannulene, Dunbar showed that among these only Cu^+ slightly prefers to bind at an η^2 edge site rather than at the center of the ring.⁵³

This preference of iron to bind to external carbon atoms can be understood by considering molecular orbitals; the bond between a transition metal (TM) and a PAH is established by the efficiency of the electronic donation/backdonation process, that is to say (i) the donation of π electrons located in the highest occupied molecular orbitals (HOMOs) of the PAH into the empty d orbitals of the TM and (ii) the backdonation of d electrons into the π^* lowest unoccupied molecular orbitals (LUMOs) of the PAH. The bond strength increases with the

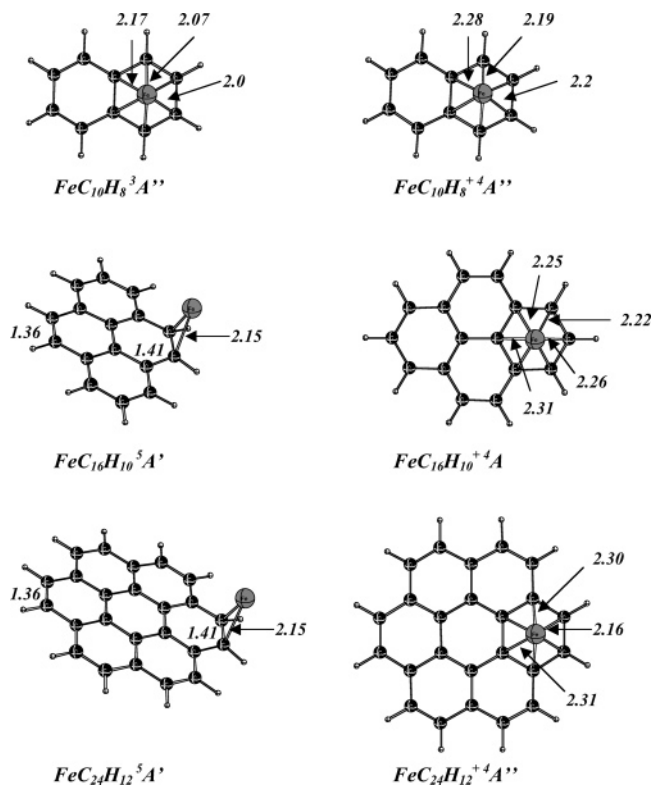


Figure 1. Structures and electronic states of the most stable Fe-PAH (left) and Fe-PAH⁺ (right) complexes for naphthalene, pyrene, and coronene found at the MPW1PW91/6-31+G(d,p) (MB2) level of theory. Iron-carbon distances are expressed in angstroms.

positive overlap between the orbitals in interaction. Dunbar⁵³ argued that this effect accounts for the distortion with respect to the expected η^6 coordination of the TM. A similar argument can be used to rationalize the fact the iron prefers to bind to the outer ring in the cases of both neutral and cationic iron-coronene complexes. In the $Fe-C_{16}H_{10}$ and $Fe-C_{24}H_{12}$ complexes, the weakening of the C-C bond resulting from an efficient donation/backdonation process is illustrated by the lengthening of the C-C bond by 0.05 Å (Figure 1).

4. Influence of the Coordination of Iron on the IR Spectra of Neutral and Cationic PAHs

As mentioned in the Introduction, many efforts have been devoted to the identification of the carriers of the astronomical AIBs. The main bands are located at 3.3, 6.2, "7.7" (a blend of several bands), 8.6, 11.3, and 12.7 μm . The 3.3 μm band is attributed to the C-H stretch, and the 6.2, "7.7", and 8.6 μm bands to the C-C stretch and in-plane (ip) C-H bends. The 6.2 μm band would correspond to quasi-pure C-C stretch, the 8.6 μm band to the ip C-H bend, and the "7.7" μm band to a mixture of both. The 11.3 and 12.7 μm bands are attributed to out-of-plane (oop) C-H vibrations. In the following, we will present and comment on the spectra of Fe-PAH complexes calculated at the MB2 level and discuss the influence of the size of the basis set. Emphasis is given to the relative band intensities for the three spectral regions at 3-4, 6-10, and 10-15 μm and on the variations of the positions of two bands, the pure C-C stretch at around 6.2 μm , and the C-H oop bend in the 11-13 μm range. Because these bands are quite well isolated from the others, they have been the subject of detailed modeling of their profiles in the astronomical literature.²⁹

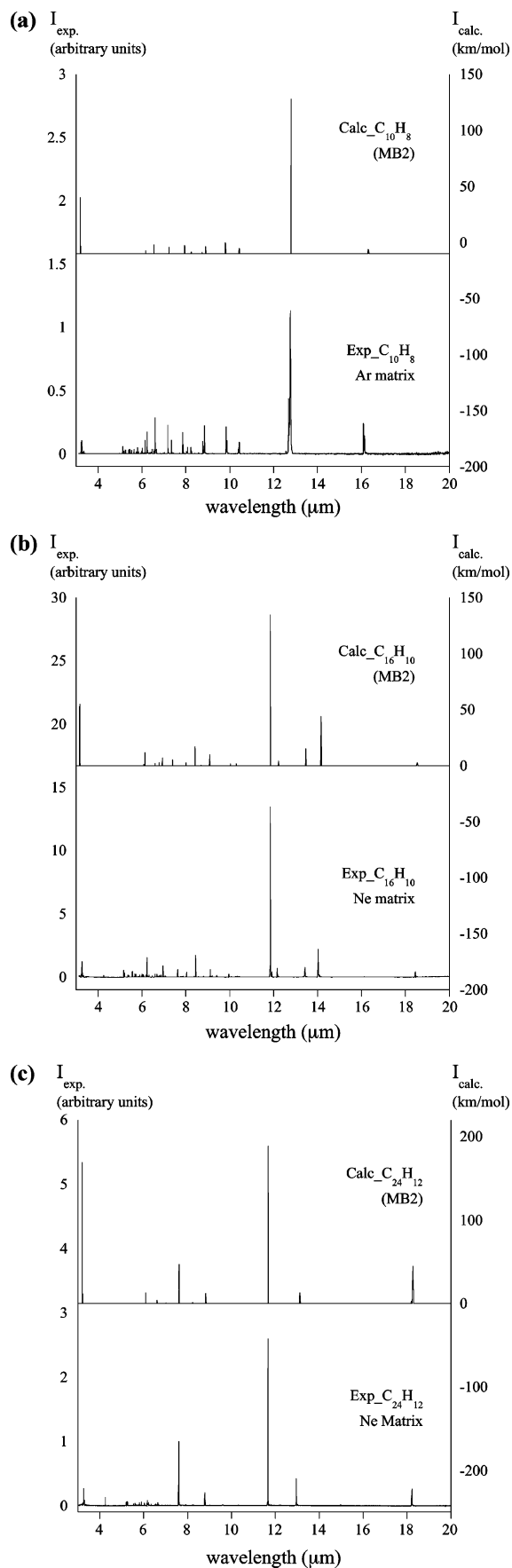


Figure 2. Comparison between IR absorption spectra calculated at the MPW1PW91/6-31+G(d,p) (MB2) level and experimental IR spectra recorded in cold matrixes ((a) argon for C_{10}H_8 ⁷¹ and (b) neon for $\text{C}_{16}\text{H}_{10}$ and (c) $\text{C}_{24}\text{H}_{12}$ ⁸). The calculated frequencies have been scaled using the appropriate factors (subsection 4.1).

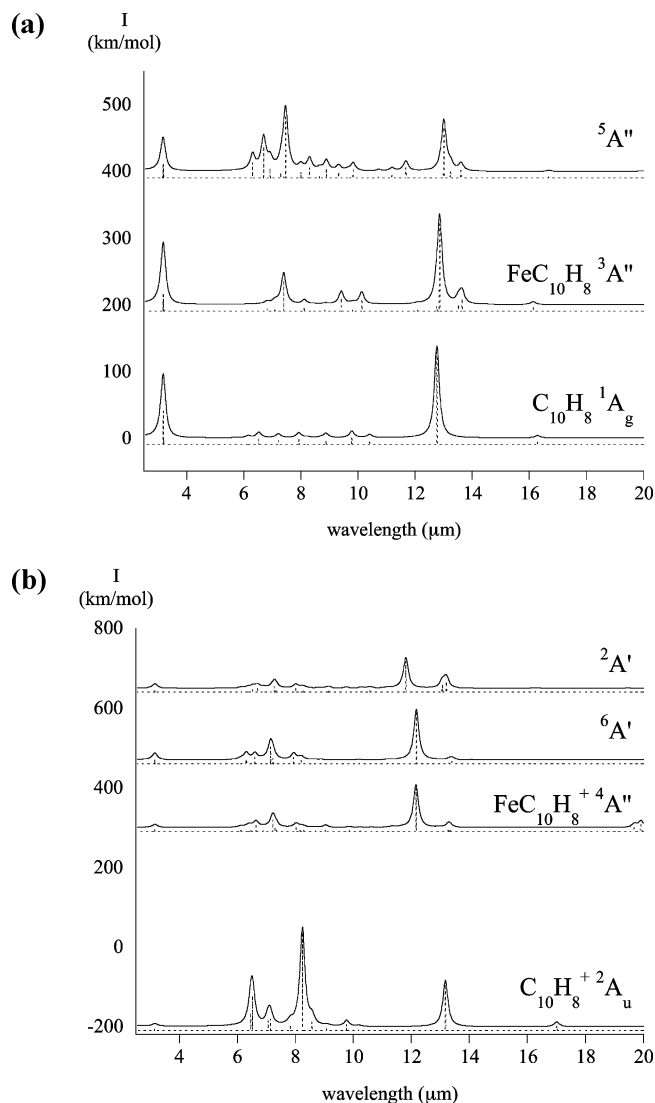


Figure 3. Calculated IR spectra of the most stable isomers of (a) neutral and (b) cationic iron–naphthalene complexes $\text{Fe}-\text{C}_{10}\text{H}_8^{0/+}$ obtained at the MPW1PW91/6-31+G(d,p) level of theory. Calculated spectra of C_{10}H_8 and $\text{C}_{10}\text{H}_8^+$ are also reported. Discrete spectra are convoluted by a Lorentzian profile with a full width at half-maximum (fwhm) of $0.2 \mu\text{m}$. Wavelengths are derived from calculated frequencies scaled by factors of 0.973 for $\lambda > 5 \mu\text{m}$ and 0.962 for $\lambda < 5 \mu\text{m}$.

4.1. Calibration. It is now well-known that scaling factors have to be applied to the calculated harmonic frequencies at the DFT level for basis set incompleteness and anharmonicity effects. We determined these scaling factors for $\text{Fe}-\text{PAH}$ and $\text{Fe}-\text{PAH}^+$ by comparing the calculated IR spectrum of the corresponding PAH to the experimental spectrum recorded in a cold matrix of argon for naphthalene⁷¹ and of neon for pyrene and coronene.⁸ Using this approach, we showed that two scaling factors had to be used, one for the $\lambda > 5 \mu\text{m}$ range and one for the $\lambda < 5 \mu\text{m}$ range, where modes of larger anharmonicity are present. The scaling factor for the $\lambda > 5 \mu\text{m}$ region was adjusted using the most intense band of the oop C–H bend, which is located at $\sim 11.6 \mu\text{m}$. The scaling factor for $\lambda < 5 \mu\text{m}$ was estimated using the most intense band of the C–H stretch at $\sim 3.3 \mu\text{m}$. The derived scaling factors are 0.973, 0.979, and 0.973 in the $\lambda > 5 \mu\text{m}$ range and 0.962, 0.947, and 0.952 in the $\lambda < 5 \mu\text{m}$ range for C_{10}H_8 , $\text{C}_{16}\text{H}_{10}$, and $\text{C}_{24}\text{H}_{12}$, respectively. Experimental and scaled calculated spectra are reported in Figure 2, showing good agreement in both band positions and intensities. Only the $3.3 \mu\text{m}$ band intensity exhibits a noticeable

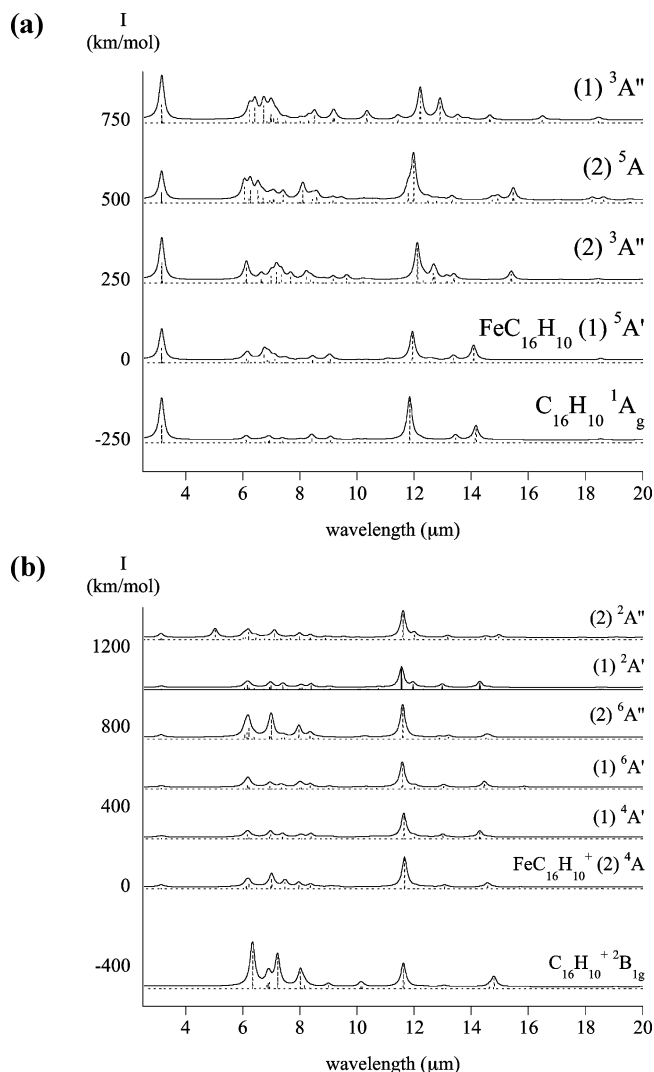


Figure 4. Calculated IR spectra of the most stable isomers of (a) neutral and (b) cationic iron-pyrene complexes $\text{Fe-C}_{16}\text{H}_{10}^{0/+}$ obtained at the MPW1PW91/6-31+G(d,p) level of theory. Calculated spectra of $\text{C}_{16}\text{H}_{10}$ and $\text{C}_{16}\text{H}_{10}^+$ are also reported. Discrete spectra are convoluted by a Lorentzian profile with a fwhm of $0.2 \mu\text{m}$. Wavelengths are derived from calculated frequencies scaled by factors of 0.979 for $\lambda > 5 \mu\text{m}$ and 0.947 for $\lambda < 5 \mu\text{m}$.

discrepancy, but this effect is well-known and has been discussed in detail by Langhoff.¹⁸

4.2. Results. The IR spectra of all calculated stable isomers of Fe-PAH and Fe-PAH⁺ are reported in Figures 3a and 3b for C_{10}H_8 , 4a and 4b for $\text{C}_{16}\text{H}_{10}$, and 5a and 5b for $\text{C}_{24}\text{H}_{12}$. The spectrum of the corresponding bare PAH^{0/+} is reported at the bottom of each figure. In this section, we will only refer to the calculated spectra of the ground states unless otherwise specified. The list of the main band positions and intensities can be found as Supporting Information. Band positions are expressed in both wavelengths and wavenumbers, and intensities are given as relative values compared with the most intense band, which is in all cases a oop C-H bending mode (cf. Table 3). The $I_{6-10\mu\text{m}}/I_{10-15\mu\text{m}}$ intensity ratios are calculated by dividing the sum of the intensities of all bands in the 6–10 μm range by the sum of the intensities of all bands in the 10–15 μm region. Such band ratios are often used to analyze astronomical spectra, and their variations are rationalized in terms of changes of neutral versus ionized PAH relative abundancies.⁴⁴

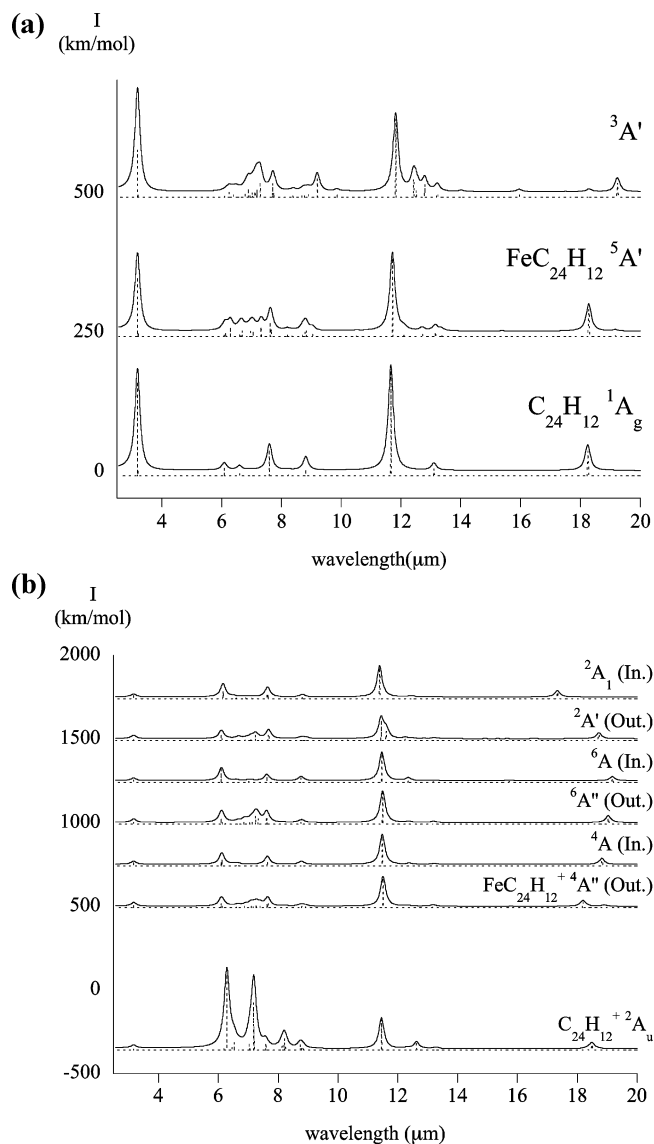


Figure 5. Calculated IR spectra of the most stable isomers of (a) neutral and (b) cationic iron-coronene complexes $\text{Fe-C}_{24}\text{H}_{12}^{0/+}$ obtained at the MPW1PW91/6-31+G(d,p) level of theory. Calculated spectra of $\text{C}_{24}\text{H}_{12}$ and $\text{C}_{24}\text{H}_{12}^+$ are also reported. Discrete spectra are convoluted by a Lorentzian profile with a fwhm of $0.2 \mu\text{m}$. Wavelengths are derived from calculated frequencies scaled by factors of 0.973 for $\lambda > 5 \mu\text{m}$ and 0.952 for $\lambda < 5 \mu\text{m}$.

The 3.3 μm bands are hardly affected by the coordination of iron, in both position and relative intensity. These bands remain intense in neutral Fe-PAH complexes and weak in cationic complexes.

The 6–10 μm region is the most affected by the coordination of iron for both neutral and cationic PAHs. Bare neutral PAHs have weak bands in this region, but the coordination of iron leads to the appearance of stronger bands, resulting in an increase of ~ 2.5 of the $I_{6-10\mu\text{m}}/I_{10-15\mu\text{m}}$ ratio (Table 3). The most striking feature of the iron coordination occurs for PAH cations with a strong decrease of the $I_{6-10\mu\text{m}}/I_{10-15\mu\text{m}}$ ratio up to a factor of 6.8 in the case of $\text{C}_{10}\text{H}_8^+$. The clear result is that the coordination of iron has a moderating effect on the intensities of the bands in the 6–10 μm region, leading to relatively close values of the $I_{6-10\mu\text{m}}/I_{10-15\mu\text{m}}$ ratios in the Fe-PAH and Fe-PAH⁺ complexes: 0.54 and 0.60 for naphthalene, 0.89 and 1.07 for pyrene, and 1.02 and 1.13 for coronene. This can be qualitatively explained in terms of partial charge transfer. These bands correspond to ip C-C stretching and C-H bending modes

TABLE 3: $I_{6-10\mu\text{m}}/I_{10-15\mu\text{m}}$ Ratios (R) for the Ground States of PAH^{0/+} and Their Complexes with Iron, the Effects of the Coordination of Iron on This Ratio, and the Effect of the Complex Charge^a

(Fe)PAH ^{0/+}	R	$R(\text{Fe-PAH}^{0/+})/R(\text{PAH}^{0/+})$	$R(\text{Fe-PAH}^+)/R(\text{Fe-PAH}^0)$	λ oop CH bend (μm (cm^{-1}))	$\delta\lambda$ oop CH bend (Fe-PAH vs PAH) (μm)	λ ip C-C stretch (μm (cm^{-1}))	$\delta\lambda$ ip C-C stretch (Fe-PAH vs PAH) (μm)
C ₁₀ H ₈	0.20			12.77 (783.1)			
FeC ₁₀ H ₈	0.54	2.70		12.86 (777.6)	+0.10	6.32 (1582.3)	
C ₁₀ H ₈ ⁺	4.10			13.17 (759.3)			
FeC ₁₀ H ₈ ⁺	0.60	0.15	1.11	12.16 (822.4)	-1.01		
C ₁₆ H ₁₀	0.35			11.85 (843.9)		6.13 (1631.3)	
FeC ₁₆ H ₁₀	0.89	2.54		11.95 (836.8)	+0.10	6.14 (1628.7)/ 6.19 (1615.5)	+0.01/+0.06
C ₁₆ H ₁₀ ⁺	3.22			11.63 (859.8)		6.35 (1574.8)/ 6.34 (1577.3)	
FeC ₁₆ H ₁₀ ⁺	1.07	0.33	1.20	11.67 (856.9)	+0.04	6.22 (1607.7)/ 6.13 (1631.3)	-0.13/-0.21
C ₂₄ H ₁₂	0.47			11.67 (856.9)		6.10 (1639.3)	
FeC ₂₄ H ₁₂	1.02	2.17		11.72 (853.2)	+0.05	6.30 (1587.3)	+0.20
C ₂₄ H ₁₂ ⁺	5.13			11.46 (872.6)		6.29 (1589.8)/ 6.19 (1615.5)	
FeC ₂₄ H ₁₂ ⁺	1.13	0.22	1.11	11.51 (868.8)	+0.05	6.10 (1639.3)/ 6.10 (1639.3)	-0.19/-0.09

^a Positions of the intense out-of-plane (oop) C-H bend and in-plane (ip) C-C stretch bands are reported, as well as the shift of these bands induced by the coordination of iron.

of the PAH. When the PAH cation coordinates to iron, there is a partial transfer of the positive charge toward iron, then less charge fluctuation is expected, leading to less intense bands. When neutral PAH coordinates to iron, electrons involved in the C-C and C-H bonds move toward iron, and the PAH becomes partially positively charged, which leads to more charge fluctuation and more intense bands.

Concerning band positions, we limit our analysis to the strong oop C-H bend in the 11–13 μm range and the pure ip C-C stretch in the 6.2 μm range. For the latter band, the comparison is only possible for complexes involving pyrene and coronene; in the naphthalene complexes, the bands occur at longer wavelengths (~ 6.5 – 6.6 μm). The derived trend appears to be a blue shift of the bands for ionized complexes and a red shift for neutral complexes. This still has to be confirmed on a larger sample of species.

As in the case of bare PAHs, the position of the most intense oop C-H bend band depends on the number of adjacent hydrogens, which varies from four in naphthalene to two in coronene. The coordination of iron mostly results in a red shift of the band by 0.04 to 0.10 μm , except in the Fe-C₁₀H₈⁺ complex for which a blue shift of 1.01 μm is calculated (cf. Table 3 and Figures 3–5). The shift of the most intense band also can be accompanied by additional spectral changes. A weak band appears at 13.65 μm (731.6 cm^{-1}) in the Fe-C₁₀H₈ complex (cf. Figure 3a). The occurrence of this small band is due to the fact that the coordination of iron on one of the two cycles breaks the symmetry; C₁₀H₈ belongs to the D_{2h} symmetry group, and Fe-C₁₀H₈ to the C_s symmetry group. Satellite bands are also observed at 13.28 and 13.33 μm (753.0 and 750.2 cm^{-1}) for the Fe-C₁₀H₈⁺ complex (Figure 3b). The most intense band located at 13.17 μm (759.3 cm^{-1}) in the spectrum of bare C₁₀H₈⁺ is blue-shifted when it coordinates to iron; it is then found at 12.16 μm (822.4 cm^{-1}) with a secondary group of bands of low intensity at 13.28 and 13.33 μm (753.0 and 750.2 cm^{-1}) (Figure 3b). It should be mentioned that this band splitting is general and is indeed the cause of the shift observed for the most intense band. As the PAH becomes larger (naphthalene \rightarrow pyrene \rightarrow coronene), one red-shifted band remains very intense whereas the others have less and less intensity. This can be intuitively understood as larger systems are less perturbed in terms of symmetry breaking by the iron atom.

For most of the studied complexes, the IR spectrum of the ground state can be distinguished from the IR spectra of the

higher-energy complexes using the band positions as well as the relative intensities. For instance, in the spectrum of the ground state of Fe-C₁₀H₈, the $I_{6-10\mu\text{m}}/I_{10-15\mu\text{m}}$ ratio is much lower (0.54 vs 2.22) than for the ⁵A' state, which was found to be quasi-degenerate (Figure 3a and Table 1). In the same vein, the ground state of Fe-C₁₆H₁₀ can be differentiated from the higher-energy isomers as more intense bands occur in the 6–10 μm range for the (2) ³A'', (2) ⁵A, and (1) ³A'' excited states with respect to the ⁵A' ground state (Figure 4a). This is also reflected by the $I_{6-10\mu\text{m}}/I_{10-15\mu\text{m}}$ ratios, which are, respectively, 1.14, 1.30, 1.59, and 0.89. For Fe-C₁₆H₁₀⁺, however, it seems hard to make the distinction between the different stable isomers except for the ⁶A'' state with the type 2 structure, which has a higher $I_{6-10\mu\text{m}}/I_{10-15\mu\text{m}}$ ratio (1.89) than the others (Figure 4b).

This detailed study brings new quantitative results on the band shifts and intensity ratio changes induced by the coordination of iron on neutral and cationic PAHs. It explores the influence of the PAH size. A simple view of the effect of metallic coordination was previously given by Ellinger et al., who generalized the results obtained for the Fe-anthracene⁺ compounds by concluding that the spectrum of an iron-PAH complex should be close to the neutral PAH spectrum.¹⁶ According to our study, this view appears to be too simplistic.

4.3. Influence of the Basis Set. The IR spectra of the ground states of Fe-PAH and Fe-PAH⁺ calculated at the MB1 and MB2 levels were compared. The calibration procedure for the calculated data is explained in subsection 4.1 and shown as an example in Figure 6a for the case of C₂₄H₁₂. The bands other than those used for calibration were found to be red-shifted. Such a red-shift effect is also systematic between calculated spectra at the MB1 level compared to those at the MB2 level. The red-shift was found to decrease when the size of the PAH increases. Figure 6b compares the two calculated spectra for Fe-C₂₄H₁₂ and Fe-C₂₄H₁₂⁺. Although some discrepancies can be observed in both band positions and intensities, they are not drastic and can be considered as acceptable given the size and complexity of the calculated species. This is encouraging for the purpose of dealing with larger systems such as Fe₂-C₂₄H₁₂⁺ and Fe-(C₂₄H₁₂)₂⁺ that previously have been studied in the gas phase^{46,47} and whose structures will be the subject of a future paper.⁷²

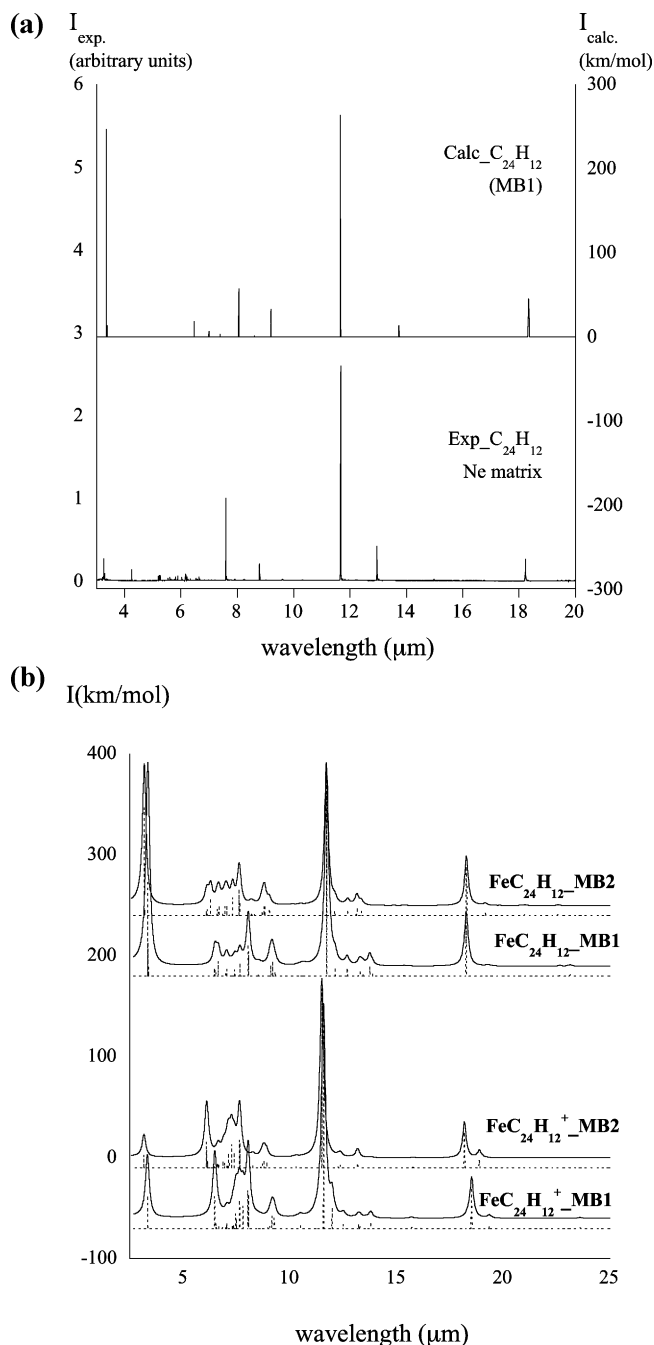


Figure 6. IR spectra calculated at the MB1 levels for coronene ($C_{24}H_{12}$) and its complexes with Fe and Fe^+ . (a) The spectrum of coronene with appropriate scaling is compared to the experimental one.⁸ (b) The spectra of the ground states of $Fe-C_{24}H_{12}^{0+}$ are compared with those calculated at the MB2 level. Wavelengths are derived from calculated frequencies using the appropriate scaling factors (subsections 4.1 and 4.3).

5. Astrophysical Implications

5.1. Thermodynamics. The binding energies between an iron atom and PAHs were found to be approximately 4 times larger for cationic PAHs (mean BDE of 2.6 eV) than those for neutral PAHs (mean BDE of 0.6 eV). This suggests that Fe-PAH complexes can survive much longer in their cationic form in the astronomical regions emitting the AIBs, which are rich in UV photons. The energy of the iron-PAH bond being lower than the typical energy of the C-H bond of a PAH (4.5–4.8 eV), the lowest-energy photodissociation pathway is therefore expected to be the loss of iron. Nanograins made of iron and

PAHs could then be good candidates for the astronomical VSGs, which have been shown to release free PAHs at the surfaces of molecular clouds under the action of UV-vis photons,^{32,44} and experiments are in progress in our laboratory to study such a scenario.⁷³

5.2. Infrared Spectroscopy. It is commonly admitted that interstellar PAHs are a mixture of neutral and charged species in a proportion that depends on the environment.^{33,74–77} Still, the relative abundancies of neutral and cationic PAHs have been estimated in only a few cases.^{32,44,78} According to our study, we can conclude that it will be very difficult to disentangle the contributions from neutral and cationic iron-PAH complexes on the basis of their band intensity ratios, which happen to be very similar in both types of complexes. Regarding band positions, Hudgins et al. put forward the idea that the incorporation of nitrogen atoms in the PAH skeleton would explain the position of the 6.2 μm band that exhibits a systematic blue shift compared with laboratory spectra.¹⁷ The authors excluded other candidates and in particular iron-PAH complexes. On the contrary, our calculations show that the latter species cannot be excluded because a significant blue shift is achieved upon coordination of a PAH^+ with iron. It also should be mentioned that the process of incorporating a nitrogen atom deep into the PAH skeleton is likely to have a large activation barrier as previously noted by van Diedenhoven et al.³³ On the contrary, the formation of iron-PAH complexes can occur without any barriers by simple association reaction between the metallic atom and the molecular PAH,^{46,49} making their formation much more likely in the ISM.

Van Diedenhoven et al. also called for the study of the influence of complexation on the C-H modes.³³ We showed that the complexation with iron induces a shift of the resonant band corresponding to the oop C-H bending mode toward longer wavelengths (subsection 4.2). This shift is however quite small, 0.04–0.10 μm (Table 3), and considering that the astronomical 11.3 μm band is quite broad due to the emission process,^{29,31} it might not be a sensitive enough diagnostic to reveal the complexation of PAHs with iron. Extension of the work to a larger sample of species could reveal other trends in the future.

6. Summary and Conclusions

The study presented in this paper is motivated by the search for alternative candidates to molecular PAHs as the emitters of the so-called aromatic infrared bands. Organometallic complexes made of iron and PAHs are good candidates because (i) they could easily form in the ISM and this would account for the depletion of iron from the gas phase and (ii) they could photodissociate, explaining the transition between very small grains and molecular-type PAH species at the UV-irradiated surface of molecular clouds.

We investigated the structures, energetics, and IR spectra of model Fe-PAH and Fe-PAH⁺ complexes using hybrid Hartree-Fock/DFT methods with two different basis sets. The considered PAHs are naphthalene ($C_{10}H_8$), pyrene ($C_{16}H_{10}$), and coronene ($C_{24}H_{12}$).

Interesting structural information was obtained. In the ground states of neutral $Fe-C_{16}H_{10}$ and $Fe-C_{24}H_{12}$, iron coordinates on top of the middle of an external C-C bond whereas it coordinates on top of the middle of an aromatic ring for $Fe-C_{10}H_8$. The latter structure was also obtained for the ground states of $Fe-C_{10}H_8^+$, $Fe-C_{16}H_{10}^+$, and $Fe-C_{24}H_{12}^+$. The iron-PAH binding energy was determined to be between 0.62 and 0.68 eV for the neutral complexes and between 2.59 and 2.77

eV for the cationic ones. Cationic species are therefore expected to survive longer in the UV-irradiated regions of the ISM. Besides, the iron-PAH⁺ binding energy being smaller than the typical CH binding energy in a PAH, we expect photodissociation to remove the iron center. If we extrapolate these results to larger complexes, then we can conclude that these species are good candidates for the astronomical VSGs that have been shown to produce molecular PAH-type species in UV-irradiated regions.^{32,44}

The only direct diagnostics for the presence of species in the ISM are their spectral fingerprints. In this paper, we show systematic effects triggered by the coordination of iron on the mid-IR spectra (3–20 μm) of the neutral and cationic PAHs mentioned above. The main effect concerns the intensities of the bands in the 6–10 μm region; these bands, intense in cationic PAHs and weak in neutral PAHs, respectively, lose and gain intensity upon the coordination of iron, which happens to have a general moderating effect. Small shifts appear in the positions of the 6.2 and 11.3 μm bands for iron-coordinated PAHs versus bare PAHs, but it is difficult to propose a firm diagnostics for the presence of such complexes in the ISM considering the uncertainty of the calculated positions and the fact that the astronomical bands are broad due to the emission process.²⁹

The work presented here is part of an ongoing effort in our group to study the properties of iron-PAH complexes in the conditions of the ISM. The calculations are performed in synergy with experiments. For example, the dissociation of X-Fe-C₂₄H₁₂⁺ complexes (X = C₅H₅ or C₅(CH₃)₃) under UV-vis irradiation and collisions was investigated with the Piège à Ions pour la Recherche et l'Étude de Nouvelles Espèces d'Intérêt Astrophysique (PIRENEA) set up, a homemade cold ion trap dedicated to astrochemistry. The results will be published in a coming paper.⁷³ The infrared spectra of these X-Fe-C₂₄H₁₂⁺ complexes were also investigated at FELIX and compared with calculated spectra.⁵¹

In the future, we plan to investigate the structures, photo-physics, and spectroscopy of larger complexes containing several PAHs and iron atoms, which are likely to be good candidates for astronomical VSGs. These studies represent both theoretical and experimental challenges. As we showed here, the effect of the basis set on the thermodynamics and IR spectra becomes smaller as the size of the PAH increases. This is encouraging for the theoretical studies of larger species, and the properties of species such as Fe-(C₂₄H₁₂)₂⁺ and Fe₂-C₂₄H₁₂⁺ will be reported in another paper.⁷² However, the theoretical treatment to describe the electronic and vibrational structures of Fe_m-PAH_n⁽⁺⁾ (m, n > 1) clusters will require the use of even less computationally costly methods.

Acknowledgment. A.S. acknowledges the Groupement Scientifique CALMIP (<http://www.calmip.cict.fr/>) of Université Toulouse 3 that allowed her to perform DFT calculations on the SOLEIL calculator. Support from the French national program, “Physique et Chimie du Milieu Interstellaire”, is also acknowledged. Finally, the referees are thanked for their useful comments that helped to improve the paper.

Supporting Information Available: Additional tables and figures. This material is available free of charge via the Internet at <http://pubs.acs.org>.

References and Notes

- Léger, A.; Puget, J. L. *Astron. Astrophys.* **1984**, *137*, L5.
- Allamandola, L. J.; Tielens, A. G.; Baker, J. R. *Astrophys. J.* **1985**, *290*, L25.
- Cook, D. J.; Schlemmer, S.; Balucani, N.; Wagner, D. R.; Harrison, J. A.; Steiner, B.; Saykally, R. J. *J. Phys. Chem. A* **1998**, *102*, 1465.
- Hudgins, D. M.; Allamandola, L. J. *J. Phys. Chem.* **1995**, *99*, 3033.
- Hudgins, D. M.; Allamandola, L. J. *J. Phys. Chem.* **1995**, *99*, 8978.
- Hudgins, D. M.; Sandford, S. A.; Allamandola, L. J. *J. Phys. Chem.* **1994**, *98*, 4243.
- Joblin, C.; Boissel, P.; Léger, A.; D'Hendecourt, L.; Defourneau, D. *Astron. Astrophys.* **1995**, *299*, 835.
- Joblin, C.; D'Hendecourt, L.; Léger, A.; Defourneau, D. *Astron. Astrophys.* **1994**, *281*, 923.
- Kim, H.-S.; Saykally, R. J. *Astrophys. J., Suppl. Ser.* **2002**, *143*, 455.
- Oomens, J.; Sartakov, B. G.; Tielens, A.; Meijer, G.; von Helden, G. *Astrophys. J.* **2001**, *560*, L99.
- Oomens, J.; Tielens, A.; Sartakov, B. G.; von Helden, G.; Meijer, G. *Astrophys. J.* **2003**, *591*, 968.
- Szczepanski, J.; Vala, M. *Nature* **1993**, *363*, 699.
- Szczepanski, J.; Vala, M. *Astrophys. J.* **1993**, *414*, 646.
- Bauschlicher, C. W., Jr.; Partridge, H.; Langhoff, S. R. *J. Phys. Chem.* **1992**, *96*, 3273.
- de Frees, D. J.; Miller, M. D.; Talbi, D.; Pauzat, F.; Ellinger, Y. *Astrophys. J.* **1993**, *408*, 530.
- Ellinger, Y.; Pauzat, F.; Lengsfeld, B. H. *J. Mol. Struct. (THEOCHEM)* **1999**, *458*, 203.
- Hudgins, D. M.; Bauschlicher, C. W.; Allamandola, L. J. *Astrophys. J.* **2005**, *632*, 316.
- Langhoff, S. R. *J. Phys. Chem.* **1996**, *100*, 2819.
- Pauzat, F.; Ellinger, Y. *Chem. Phys.* **2002**, *280*, 267.
- Pauzat, F.; Talbi, D.; Ellinger, Y. *Astron. Astrophys.* **1995**, *293*, 263.
- Pauzat, F.; Talbi, D.; Ellinger, Y. *Astron. Astrophys.* **1997**, *319*, 318.
- Malloci, G.; Joblin, C.; Mulas, G. *Astron. Astrophys.* **2006**, *462*, 627.
- Malloci, G.; Joblin, C.; Mulas, G. *Chem. Phys.* **2007**, *332*, 353.
- Allamandola, L. J.; Hudgins, D. M.; Sandford, S. A. *Astrophys. J.* **1999**, *511*, L115.
- Bakes, E. L. O.; Tielens, A. G. G. M. *Astrophys. J.* **1994**, *427*, 822.
- Bakes, E. L. O.; Tielens, A. G. G. M.; Bauschlicher, C. W., Jr. *Astrophys. J.* **2001**, *556*, 501.
- Boulanger, F.; Boissel, P.; Cesarsky, D.; Ryter, C. *Astron. Astrophys.* **1998**, *339*, 194.
- Hony, S.; Van Kerckhoven, C.; Peeters, E.; Tielens, A.; Hudgins, D. M.; Allamandola, L. J. *Astron. Astrophys.* **2001**, *370*, 1030.
- Pech, C.; Joblin, C.; Boissel, P. *Astron. Astrophys.* **2002**, *388*, 639.
- Schutte, W. A.; Tielens, A. G. G. M.; Allamandola, L. J. *Astrophys. J.* **1993**, *415*, 397.
- Verstraete, L.; Pech, C.; Moutou, C.; Sellgren, K.; Wright, C. M.; Giard, M.; Leger, A.; Timmermann, R.; Drapatz, S. *Astron. Astrophys.* **2001**, *372*, 981.
- Rapacioli, M.; Joblin, J.; Boissel, P. *Astron. Astrophys.* **2005**, *429*, 193.
- van Diedenhoven, B.; Peeters, E.; Van Kerckhoven, C.; Hony, S.; Hudgins, D. M.; Allamandola, L. J.; Tielens, A. *Astrophys. J.* **2004**, *611*, 928.
- Peeters, E.; Hony, S.; Van Kerckhoven, C.; Tielens, A.; Allamandola, L. J.; Hudgins, D. M.; Bauschlicher, C. W. *Astron. Astrophys.* **2002**, *390*, 1089.
- Serra, G.; Chaudret, B.; Saillard, Y.; Le Beuze, A.; Rabaa, H.; Ristorcelli, I.; Klotz, A. *Astron. Astrophys.* **1992**, *260*, 489.
- Chaudret, B.; Le Beuze, A.; Rabaa, H.; Saillard, Y.; Serra, G. *New J. Chem.* **1991**, *15*, 791.
- Ristorcelli, I.; Klotz, A. *Astron. Astrophys.* **1997**, *317*, 962.
- Marty, P.; de Parseval, P.; Klotz, A.; Chaudret, B.; Serra, G.; Boissel, P. *Chem. Phys. Lett.* **1996**, *256*, 669.
- Marty, P.; de Parseval, P.; Klotz, A.; Serra, G.; Boissel, P. *Astron. Astrophys.* **1996**, *316*, 270.
- Cassam-Chenai, P. *Planet. Space Sci.* **2002**, *50*, 871.
- Marty, P.; Serra, G.; Chaudret, B.; Ristorcelli, I. *Astron. Astrophys.* **1994**, *282*, 916.
- Klotz, A.; Marty, P.; Boissel, P.; Serra, G.; Chaudret, B.; Daudey, J. P. *Astron. Astrophys.* **1995**, *304*, 520.
- Rodríguez, M. *Astron. Astrophys.* **2002**, *389*, 556.
- Berné, O.; Joblin, C.; Deville, Y.; Smith, J. D.; Rapacioli, M.; Bernard, J. P.; Thomas, J.; Reach, W.; Abergel, A. *Astron. Astrophys.* **2007**, *469*, 575.
- Rapacioli, M.; Calvo, F.; Joblin, C.; Parneix, P.; Toubanc, D.; Spiegelman, F. *Astron. Astrophys.* **2006**, *460*, 519.
- Pozniak, B. P.; Dunbar, R. C. *J. Am. Chem. Soc.* **1997**, *119*, 10439.

- (47) Buchanan, J. W.; Reddic, J. E.; Grieves, G. A.; Duncan, M. A. *J. Phys. Chem. A* **1998**, *102*, 6390.
- (48) Senapati, L.; Nayak, S. K.; Rao, B. K.; Jena, P. *J. Chem. Phys.* **2003**, *118*, 8671.
- (49) Elustondo, E.; Dalibart, M.; Deroult, J.; Mascetti, J. *Phys. Chem. Earth, Part C: Sol. Terr. Planet. Sci.* **1999**, *24*, 583.
- (50) Szczepanski, J.; Wang, H.; Vala, M.; Tielens, A. G. G. M.; Eyler, J. R.; Oomens, J. *Astrophys. J.* **2006**, *646*, 666.
- (51) Simon, A.; Joblin, C.; Polfer, N.; Oomens, J., to be submitted for publication.
- (52) Bauschlicher, C. W., Jr.; Bakes, E. L. O. *Chem. Phys.* **2000**, *262*, 285.
- (53) Dunbar, R. C. *J. Phys. Chem. A* **2002**, *106*, 9809.
- (54) Klippenstein, S. J.; Yang, C.-N. *Int. J. Mass Spectrom.* **2000**, *201*, 253.
- (55) Kandalam, A. K.; Rao, B. K.; Jena, P. *J. Phys. Chem. A* **2005**, *109*, 9220.
- (56) Stevens, P. J.; Devlin, F. J.; Chabrowski, C. F.; Frisch, M. J. *J. Phys. Chem. A* **1994**, *98*, 11623.
- (57) Hay, P. J.; Wadt, W. R. *J. Chem. Phys.* **1985**, *82*, 270.
- (58) Simon, A.; Jones, W.; Ortega, J. M.; Boissel, P.; Lemaire, J.; Maitre, P. *J. Am. Chem. Soc.* **2004**, *126*, 11666.
- (59) Pathak, B.; Pandian, S.; Hosmane, N.; Jemmis, A. D. *J. Am. Chem. Soc.* **2006**, *128*, 10915.
- (60) Chang, C.; Patzer, A. B. C.; Sedlmayr, E.; Sülzle, D.; Steinke, T. *Comput. Mater. Sci.* **2006**, *35*, 387.
- (61) Chang, C.; Patzer, A. B. C.; Sedlmayr, E.; Sülzle, D. *Phys. Rev. B* **2005**, *72*, 235402.
- (62) Adamo, C.; Barone, V. *Chem. Phys. Lett.* **1997**, *274*, 242.
- (63) Adamo, C.; Barone, V. *J. Chem. Phys.* **1998**, *108*, 664.
- (64) Dunbar, R. C. *J. Phys. Chem. A* **2002**, *106*, 7328.
- (65) Frisch, M. J.; Trucks, G. W.; Schlegel, H. B.; Scuseria, G. E.; Robb, M. A.; Cheeseman, J. R.; Montgomery, J. A., Jr.; Vreven, T.; Kudin, K. N.; Burant, J. C.; Millam, J. M.; Iyengar, S. S.; Tomasi, J.; Barone, V.; Mennucci, B.; Cossi, M.; Scalmani, G.; Rega, N.; Petersson, G. A.; Nakatsuji, H.; Hada, M.; Ehara, M.; Toyota, K.; Fukuda, R.; Hasegawa, J.; Ishida, M.; Nakajima, T.; Honda, Y.; Kitao, O.; Nakai, H.; Klene, M.; Li, X.; Knox, J. E.; Hratchian, H. P.; Cross, J. B.; Bakken, V.; Adamo, C.; Jaramillo, J.; Gomperts, R.; Stratmann, R. E.; Yazyev, O.; Austin, A. J.; Cammi, R.; Pomelli, C.; Ochterski, J. W.; Ayala, P. Y.; Morokuma, K.; Voth, G. A.; Salvador, P.; Dannenberg, J. J.; Zakrzewski, V. G.; Dapprich, S.; Daniels, A. D.; Strain, M. C.; Farkas, O.; Malick, D. K.; Rabuck, A. D.; Raghavachari, K.; Foresman, J. B.; Ortiz, J. V.; Cui, Q.; Baboul, A. G.; Clifford, S.; Cioslowski, J.; Stefanov, B. B.; Liu, G.; Liashenko, A.; Piskorz, P.; Komaromi, I.; Martin, R. L.; Fox, D. J.; Keith, T.; Al-Laham, M. A.; Peng, C. Y.; Nanayakkara, A.; Challacombe, M.; Gill, P. M. W.; Johnson, B.; Chen, W.; Wong, M. W.; Gonzalez, C.; Pople, J. A. *Gaussian 03*, revision B.02; Gaussian, Inc.: Wallingford, CT, 2004.
- (66) Boys, S. F.; Bernardi, F. *Mol. Phys.* **1970**, *19*, 553.
- (67) Simon, S.; Durand, M.; Dannenberg, J. J. *J. Chem. Phys.* **1996**, *105*, 11024.
- (68) Feller, D. *Chem. Phys. Lett.* **2000**, *322*, 543.
- (69) Buchanan, J. W.; Grieves, G. A.; Reddic, J. E.; Duncan, M. A. *Int. J. Mass Spectrom.* **1999**, *183*, 323.
- (70) Meyer, F.; Khan, F. A.; Armentrout, P. B. *J. Am. Chem. Soc.* **1995**, *117*, 9740.
- (71) Hudgins, D. M.; Sandford, S. A. *J. Phys. Chem. A* **1998**, *102*, 329.
- (72) Chang, C.; Patzer, A. B. C.; Sülzle, D.; Sedlmayr, E.; Simon, A.; Joblin, C., to be submitted for publication.
- (73) Simon, A.; Joblin, C., to be submitted for publication.
- (74) Bakes, E. L. O.; Tielens, A. G. G. M.; Bauschlicher, C. W., Jr.; Hudgins, D. M.; Allamandola, L. J. *Astrophys. J.* **2001**, *560*, 261.
- (75) Le Page, V.; Snow, T. P.; Bierbaum, V. M. *Astrophys. J.* **2003**, *584*, 316.
- (76) Ruitkamp, R.; Cox, N. L. J.; Spaans, M.; Kaper, L.; Foing, B. H.; Salama, F.; Ehrenfreund, P. *Astron. Astrophys.* **2005**, *432*, 515.
- (77) Visser, R.; Geers, V. C.; Dullemond, C. P.; Augereau, J.-C.; Pontoppidan, K. M.; van Dishoeck, E. F. *Astron. Astrophys.*, in press.
- (78) Flagey, N.; Boulanger, F.; Verstraete, L.; Miville Deschênes, M. A.; Noriega Crespo, A.; Reach, W. T. *Astron. Astrophys.* **2006**, *453*, 969.
- (79) *NIST Chemistry WebBook*; Linstrom, P. J., Mallard, W. G., Eds.; National Institute of Standards and Technology: Gaithersburg MD, 2005.
- (80) *NIST Atomic Spectra Database*, version 3.1.2; Ralchenko, Y., Jou, F.-C., Kelleher, D. E., Kramida, A. E., Musgrove, A., Reader, J., Wiese, W. L., Olsen, K., Eds.; National Institute of Standards and Technology: Gaithersburg, MD, 2007.